Analysis of Eigenspace Dynamics with Applications to Array Processing

Lisa M. Zurk
Electrical and Computer Engineering Department, Portland State University
1900 SW 4th Ave
Portland, OR 97207, USA
phone: (503) 725-5423, email: zurkl@cecs.pdx.edu

Jorge E. Quijano
School of Earth and Ocean Sciences, University of Victoria
3800 Finnerty Road, Victoria BC, Canada
phone: (250) 472-4685, email: jorgeq@uvic.ca

Grant Number: N00014-13-1-0101

LONG-TERM GOALS

For an *N*-element array (Fig.1(a)), methods such as beamforming and singular value decomposition rely on estimation of the sample covariance matrix, computed from *M* independent data snapshots. As $M \to \infty$, the sample covariance is a consistent estimator of the true population covariance. However, this ideal condition cannot be met in most practical situations,[1-2] in which large-aperture arrays operate in the presence of fast maneuvering interferers, or with towed/drifting arrays strongly affected by deformation or array-depth perturbations. The long-term goal of this effort is the development of physically motivated models to statistically describe the eigenstructure (eigenvalues and eigenvectors) of sample covariance matrices in sample-starved settings, and the use of those models for performance analysis and improvement of array processing methods. To this end, mathematical tools developed in the context of Random Matrix Theory (RMT)[3-6] (mostly focused in the regime *N*~*M*) and High Dimension, Low Sample Size (HDLSS) array processing[7-8] (which considers *N*>>*M*) are applied to obtain statistical descriptions of sample eigenvalues/eigenvectors and how those quantities differ from the (true) population eigenpairs. Additional long-term goals are exploiting the information carried by sample eigenvectors for the improvement of estimators of the sample covariance matrix (i.e., signal versus noise subspaces), and for quantifying local stationary in array data (Fig.1 (b)).

OBJECTIVES

- Developing beamforming techniques for snapshot-deficient scenarios with moving targets such as the one illustrated in Fig.1. Unlike previous research, this work incorporates asymptotic results[3-8] for the sample eigenvectors and how they deviate from their true population eigenvectors.
- Developing multi-hypothesis tests for estimation of parameters such as azimuth and power of targets in the watercolumn, number of targets, and their speed, based on asymptotic limits for the sample eigenvalues, sample eigenvectors, and eigenspace projections for *N*>>*M*. A key component of this research is the analysis of the impact of source movement (i.e., time-dependent position) on the eigenspaces associated to signal and background noise.

Report Documentation Page

Form Approved
OMB No. 0704-0188

1. REPORT DATE	2. REPORT TYPE	3. DATES COVERED
30 SEP 2014		**00-00-2014 to 00-00-2014**

4. TITLE AND SUBTITLE	5a. CONTRACT NUMBER
Analysis of Eigenspace Dynamics with Applications to Array Processing	5b. GRANT NUMBER
	5c. PROGRAM ELEMENT NUMBER
6. AUTHOR(S)	5d. PROJECT NUMBER
	5e. TASK NUMBER
	5f. WORK UNIT NUMBER
7. PERFORMING ORGANIZATION NAME(S) AND ADDRESS(ES) **Portland State University,Department of Electrical and Computer Engineering,1900 SW 4th Ave,Portland,OR,97207**	8. PERFORMING ORGANIZATION REPORT NUMBER
9. SPONSORING/MONITORING AGENCY NAME(S) AND ADDRESS(ES)	10. SPONSOR/MONITOR'S ACRONYM(S)
	11. SPONSOR/MONITOR'S REPORT NUMBER(S)

12. DISTRIBUTION/AVAILABILITY STATEMENT
Approved for public release; distribution unlimited

13. SUPPLEMENTARY NOTES

14. ABSTRACT

15. SUBJECT TERMS

16. SECURITY CLASSIFICATION OF:			17. LIMITATION OF ABSTRACT	18. NUMBER OF PAGES	19a. NAME OF RESPONSIBLE PERSON
a. REPORT	b. ABSTRACT	c. THIS PAGE			
unclassified	**unclassified**	**unclassified**	**Same as Report (SAR)**	**12**	

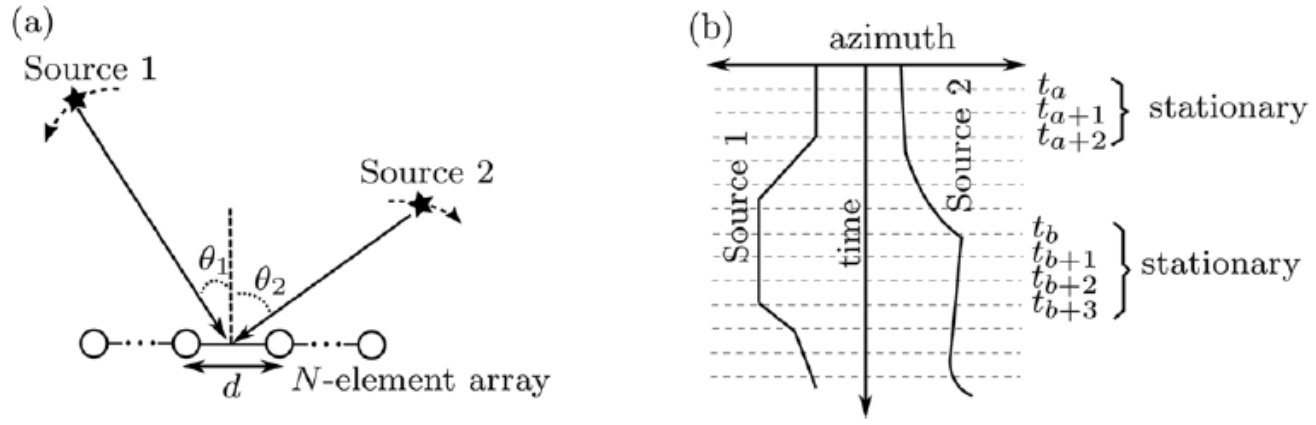

Figure 1 (a) Experimental scenario considered in this research,[9] consisting of multiple maneuvering sources detected by an N-element array after collecting M snapshots. This work considers array processing tools for cases in which N>>M. (b) Data snapshots are collected at discrete times t_a, t_{a+1}, etc. Data local stationarity occurs at time intervals of little or no variation of target azimuth (e.g., $t_a<t<t_{a+2}$ and $t_b<t<t_{b+3}$).

- Developing statistical methods for data segmentation into intervals with local stationarity[9-10] as shown in Fig. 1(b), capable of distinguishing between true variations in the covariance structure (due to underlying time-varying statistics), as opposed to variations introduced by the lack of data snapshots. Since estimation of the sample covariance matrix assumes local stationarity of the data, this segmentation approach will provide a bound for the largest number of snapshots to be included while estimating covariances.
- Obtaining an eigenvector-based estimator of the signal subspace[11] to improve the performance of subspace array processing methods. In previous ONR-sponsored work, determining the signal subspace has been carried out by defining eigenvalue-based rank estimators.[5] In contrast, the work presented here considers the benefits of including the information carried by sample eigenvectors.

APPROACH

1) Defining a snapshot model:[1] Let

$$\mathbf{y}_m \equiv \sum_{q=1}^{\hat{Q}} \mathbf{v}_{qm}\gamma_{qm} + \mathbf{w}_m; \qquad (1)$$

be a data snapshot at time t_m at an N-element array, where $\mathbf{w}_m$ is the $Nx1$ vector corresponding to the background noise of power level σ_w^2, γ_{qm} is a complex zero-mean Gaussian distributed random variable with variance σ_q^2 representing the source level of the q^{th} target in the watercolumn (see Fig.1(a)), and $\mathbf{v}_{qm}$ is the azimuth-dependent replica vector for the q^{th} target, defined as

$$\mathbf{v}_{qm} \equiv \mathbf{v}_{qm}(\theta_m) = \left[1 \;\; \exp\left(i \frac{\omega\, d \sin\theta_m}{c_o} \right) \ldots \exp\left(i \frac{\omega\, d (N-1) \sin\theta_m}{c_o} \right) \right]^T / \sqrt{N} \qquad (2)$$

where ω is the frequency in radians/s, d is the array inter-element spacing, and c_o is the water sound speed. The population covariance at time t_a is

$$\mathbf{R}_a = \sum_{q=1}^{\hat{Q}} \sigma_q^2 \mathbf{v}_{qa}^H \mathbf{v}_{qa} + \sigma_w^2 \mathbf{I}_N = \underbrace{\sum_{n=1}^{\tilde{Q}} \lambda_{na} \mathbf{u}_{na}^H \mathbf{u}_{na}}_{loud\ targets} + \underbrace{\sum_{n=\tilde{Q}+1}^{\hat{Q}} \lambda_{na} \mathbf{u}_{na}^H \mathbf{u}_{na}}_{quiet\ targets} + \underbrace{\sum_{n=\hat{Q}+1}^{\min(N,M)} \lambda_{na} \mathbf{u}_{na}^H \mathbf{u}_{na}}_{noise} \;. \qquad (3)$$

Using eq.(3), data realizations (i.e., M snapshots) can be generated from complex normally distributed vectors $\mathbf{z}$ as $\mathbf{x}_m = \mathbf{R}_a^{1/2} \mathbf{z}$. The simulated data obtained by this approach is used to study the behavior of the sample covariance matrix, estimated as:[1-2]

$$\hat{\mathbf{R}}_{Ma} = \frac{1}{M} \mathbf{X}_{Ma} \mathbf{X}_{Ma}^H; \qquad \text{with} \quad \mathbf{X}_{Ma} = \left[\mathbf{x}_a \;\; \mathbf{x}_{a+1} \cdots \mathbf{x}_{a+M-1} \right]^H \qquad (4).$$

From eq. (3), the relative impact of $\hat{Q}$, $\tilde{Q}$, σ_q^2 / σ_w^2, N, and M on the behavior of sample eigenvalues ($\hat{\lambda}_1 \ldots \hat{\lambda}_N$) and sample eigenvectors ($\hat{\mathbf{u}}_1 \ldots \hat{\mathbf{u}}_N$) will be analyzed by Monte Carlo studies and contrasted to predictions from RMT[3-6] and HDLSS.[7-8]

2) Quantifying eigenspace dynamics:[9-10,11] eigenspaces are defined as the vector space spanned by $\tilde{Q}$ eigenvectors. Signal stationarity can be quantified by tracking time-dependent variations in the eigenspace defined by target-related population eigenvectors, as illustrated in Fig. 2. In this example the decision of data stationarity is based on whether the population eigenvectors have changed direction over time (i.e., $\mathbf{u}_{1a} = \mathbf{u}_{1b}$ and $\mathbf{u}_{2a} = \mathbf{u}_{2b}$) or not. Since population eigenvectors are not observable variables, an eigenspace distance based on sample eigenvectors is defined as:[9-10]

$$r_{ab} = \left[\frac{\tilde{Q} - s_{ab}}{\tilde{Q}} \right]; \quad \text{where} \quad s_{ab} = \text{trace}\left(\left| \left[\hat{\mathbf{u}}_{1a} \; \hat{\mathbf{u}}_{2a} \ldots \hat{\mathbf{u}}_{\tilde{Q}a} \right]^H \left[\hat{\mathbf{u}}_{1b} \; \hat{\mathbf{u}}_{2b} \ldots \hat{\mathbf{u}}_{\tilde{Q}b} \right] \right|^2 \right), \qquad (5)$$

which has bounds $0 \le r_{ab} \le 1$ since the trace operator is bounded between 0 and 1. $r_{ab} = 0$ occurs when the eigenspaces at times t_a and t_b are perfectly lined up indicating data stationarity. On the other hand, $r_{ab} = 1$ results when such eigenspaces are orthogonal to each other, indicating data non-stationarity. A statistical decision rule for data stationarity can be stated as the complementary hypothesis

$$\begin{aligned} H_0 &: \text{stationary data} \rightarrow -L \le r_{ab} \le +L \\ H_1 &: \text{non stationary data} \rightarrow -L > r_{ab} \text{ or } r_{ab} > +L \end{aligned} \;, \qquad (6)$$

where the stationarity bounds $\pm L = \mu_r \pm \sigma_r$ are a function of the theoretical mean (μ_r) and standard deviation (σ_r) of r_{ab}. Based on theoretical results from HDLSS[8-9] it is possible to obtain theoretical expressions for these quantities on the assumption of data stationarity (hypothesis H_0).

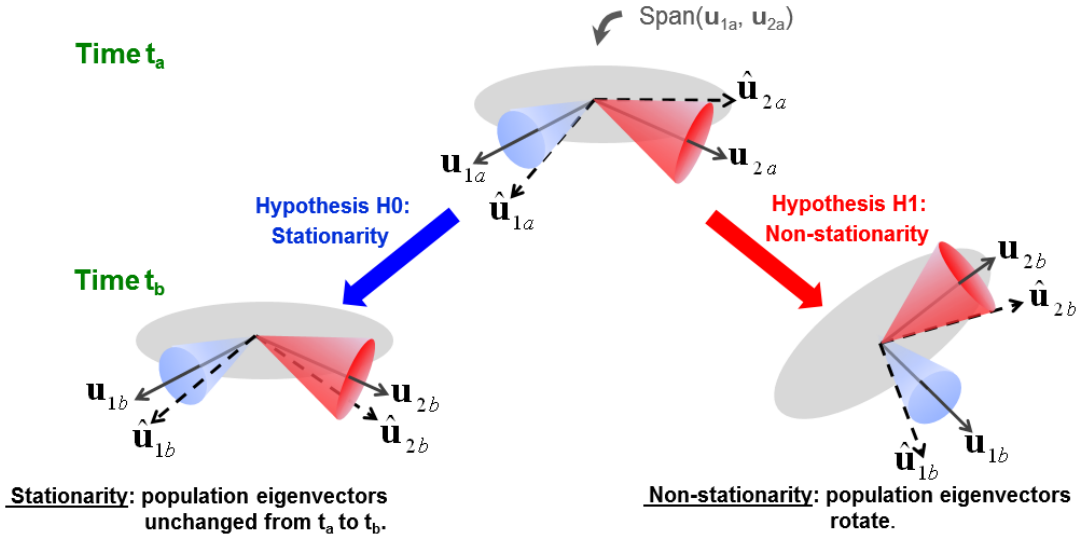

Figure 2 Illustration of the data stationarity test proposed in this work,[9-10] which consists on tracking variations in the direction of population eigenvectors at times t_a and t_b. Since population eigenvectors are not observable quantities, eigenspace variability can be tracked using the eigenspace distance metric in eq.(5), based on observable sample eigenvectors.

3) Obtaining an eigenvector-based estimator for signal and noise subspaces:[10] Subspace beamforming techniques rely on projecting noisy data snapshots into reduced rank signal eigenspaces. In this work, we consider the statistic properties of entirely random eigenspaces to identify specific eigenvectors with signal-bearing information. To explain this concept, consider the following Monte Carlo experiment illustrated in Fig. 3: given an N-dimensional sphere, randomly select K vectors and measure the angle α between these vectors and an arbitrary reference vector (shown in red). It can be shown[10,12-14] that for random vectors (i.e., vectors with no information content), the angle $\alpha_{\min} = \min(\alpha_1,...,\alpha_K)$ has a probability distribution function[10]

$$f_{\min}(\alpha_{\min}) = K\left[1-\frac{(\sin\alpha_{\min})^{2N-1}}{2N-1}\right]^{K-1}(\sin\alpha_{\min})^{2N-2}\cos\alpha_{\min} \qquad 0 \le \alpha_{\min} \le \pi/2\,. \qquad (7)$$

This concept can be extended to K eigenvectors estimated from data snapshots collected at an N-sensor array: sample eigenvectors corresponding to noise-only data exhibit the same statistics as eq.(7), while signal-bearing eigenvectors result into left-skewed distributions, as illustrated in Fig. 3. Therefore, eigenvectors with $\alpha_{\min}$ lower than a user-defined threshold should be considered as potentially "informative". In this work, we propose an algorithm described below that utilized this criteria for estimation of the signal subspace prior to beamforming.

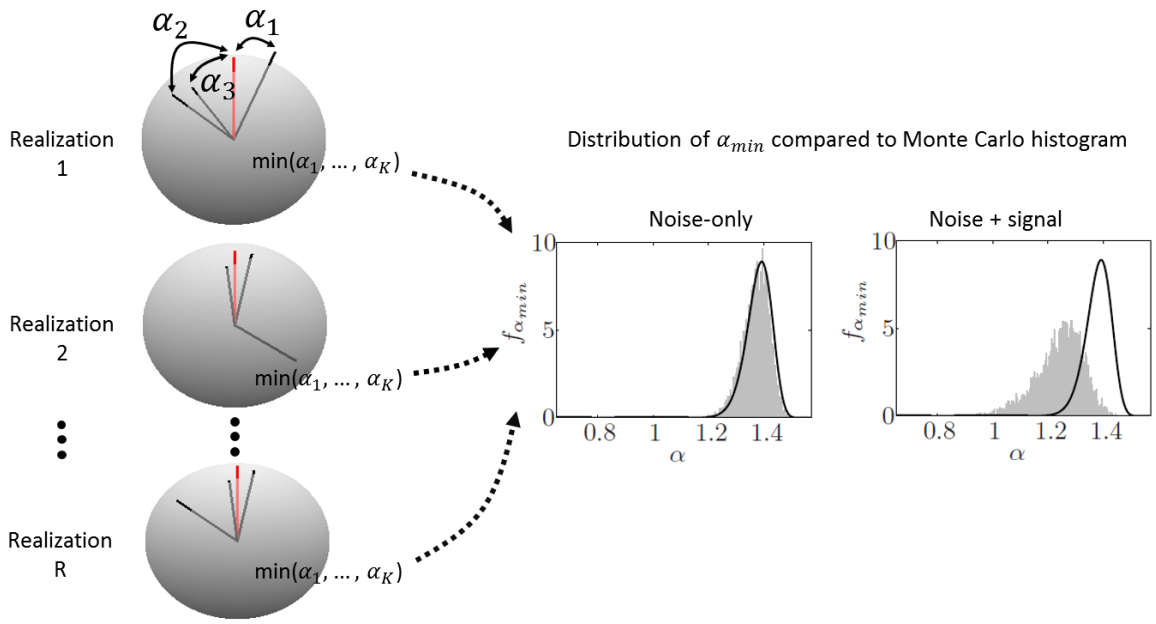

Figure 3 Example of the approach proposed in this work to identify signal-bearing vectors:[10] the minimum angle between a set of K=3 noise-only N-dimensional vectors and a reference vector (red) exhibits different behavior than the angle resulting from signal-bearing vectors (i.e., those vectors with structure that resemble the reference). In this research, this concept is extended to sample eigenvectors as a tool to estimate the signal subspace, as well as its complementary noise subspace.

WORK COMPLETED

1) An eigenvector-based metric to quantify data stationarity[9] (based on the concept illustrated in Fig.2) was proposed for an experimental scenario consisting of a single dominant interferer and multiple quiet targets of interest. A generalization of this approach to the case of $\tilde{Q}$ dominant interferers has also been proposed[10] and the theoretical results have been applied to improving a reduced rank beamformer and applied to simulated and experimental data.

2) A sample eigenvector-based estimator for the signal subspace has been proposed[10] based on the idea illustrated in Fig. 3. Beamforming results with simulated data illustrate application of this theoretical result to improve target detection in snapshot-starved scenarios.

Examples of results corresponding to applications #1 and #2 are shown in the next section.

RESULTS

The array processing techniques developed in this research have application to the improvement of subspace beamforming processors, in which the data snapshots are projected into particular subspaces of interest such as

$$\mathbf{y}_m^{(.)} = \mathbf{P}^{(.)}\,\mathbf{x}_m \ , \qquad (8)$$

where $\mathbf{P}^{(.)}$ is a subspace projection operator obtained from sample or population eigenvectors, defined in Table 1 for several cases of study.

Table 1: Definition of three data projectors $\mathbf{P}^{(.)}$ ***and adaptive beamforming weight vectors*** $\mathbf{w}^{(.)}(\theta)$ ***used in this report for comparison of array processing techniques.***

Projector	Adaptive weights	Description
$\mathbf{P}^{(true)} = \sum_{n=1}^{\hat{Q}} \mathbf{u}_n \mathbf{u}_n^H$	$\mathbf{w}^{(true)}(\theta) = \left[\mathbf{v}^H(\theta)\mathbf{R}_{(true)}^{-1}\mathbf{v}(\theta)\right]^{-1}\mathbf{R}_{(true)}^{-1}\mathbf{v}(\theta)$ $\mathbf{R}_{(true)} = \frac{1}{M}\sum_{m=a}^{a+M-1} \mathbf{y}_m^{(true)}\left[\mathbf{y}_m^{(true)}\right]^H + 10^{WNGC/10}$	Projection into true signal eigenspace. Used as benchmark for simulations
$\mathbf{P}^{(M_o)} = \sum_{n=1}^{\widetilde{Q}} \hat{\mathbf{u}}_n(M_o)\hat{\mathbf{u}}_n^H(M_o)$	$\mathbf{w}^{(M_o)}(\theta) = \left[\mathbf{v}^H(\theta)\mathbf{R}_{(M_o)}^{-1}\mathbf{v}(\theta)\right]^{-1}\mathbf{R}_{(M_o)}^{-1}\mathbf{v}(\theta)$ $\mathbf{R}_{(M_o)} = \frac{1}{M_o}\sum_{m=a}^{a+M_o-1} \mathbf{y}_m^{(M_o)}\left[\mathbf{y}_m^{(M_o)}\right]^H + 10^{WNGC/10}$	Projection into rank $\widetilde{Q}$ subspace. Sample eigenvectors estimated from M_o snapshots.
$\mathbf{P}^{(EVB)} = \sum_{n=1}^{\overline{Q}} \overline{\mathbf{u}}_n \overline{\mathbf{u}}_n^H$	$\mathbf{w}^{(EVB)}(\theta) = \left[\mathbf{v}^H(\theta)\mathbf{R}_{(EVB)}^{-1}\mathbf{v}(\theta)\right]^{-1}\mathbf{R}_{(EVB)}^{-1}\mathbf{v}(\theta)$ $\mathbf{R}_{(EVB)} = \frac{1}{M}\sum_{m=a}^{a+M-1} \mathbf{y}_m^{(EVB)}\left[\mathbf{y}_m^{(EVB)}\right]^H + 10^{WNGC/10}$	Projection into rank $\overline{Q}$ subspace. Orthonormal basis $\overline{\mathbf{u}}_n$ estimated by the algorithm described below.

Once the adaptive weights have been obtained (see Table 1), beamforming results have the form

$$BF_{Ma}^{(.)}(\theta) = \left(\mathbf{w}^{(.)}(\theta)\right)^H \hat{\mathbf{R}}_{Ma}\mathbf{w}^{(.)}(\theta) \ . \qquad (9)$$

This report discusses two beamforming approaches that exploit either data stationarity or signal information content in sample eigenvectors:

1) Stationarity-aided beamforming:[9-10] Application of the stationarity metric in eq.(5) for improvement on the estimation of adaptive beamforming weights is demonstrated in this section with simulated and experimental data. The simulated setting allows to compare the benchmark beamformer $BF_{Ma}^{(true)}$ to $BF_{Ma}^{(M_o=M)}$, which is the traditional MVDR adaptive beamformer with white noise gain constraint. This is also contrasted to $BF_{Ma}^{(M_o \geq M)}$ in which M_o is determined according to the data stationarity criterion in eq.(6). The simulated example consists of two loud interferers (20 dB and 25 dB) and four quiet sources with powers ranging between 2 dB and 5 dB above the noise level of 0 dB. Figure 3 (a) shows target azimuths as a function of time. The data stationarity criterion in Fig.3(b) is dominated by the loud interferers, so $\widetilde{Q} = 2$ in eq.(5). This is evident for 0<t<130 s, for which both interferers have constant azimuth, resulting in a large interval of data stationarity. Another interesting feature is observed around 450 s, where both interferers are undistinguishable as a result of being located at the same azimuth. In this case, $\widetilde{Q} = 1$ and eq.(5) predicts accurately a sharp drop of the stationarity metric. Figure 3(c) shows the benchmark beamformer $BF_{Ma}^{(true)}$, in which all targets can be clearly visualized. Figure 3(d) shows $BF_{Ma}^{(M_o=M)}$, obtained by estimating the adaptive weights using M=10 snapshots at each time. Compared to panel (c), noise levels are higher and target angular resolution is lower. Figure 3(e) shows the improved results obtained by estimating beamforming weights using $M_o \geq 10$ snapshots according to the data stationarity bounds in Fig.3 (b). The results resemble those in panel (c), with similar background noise level and angular resolution.

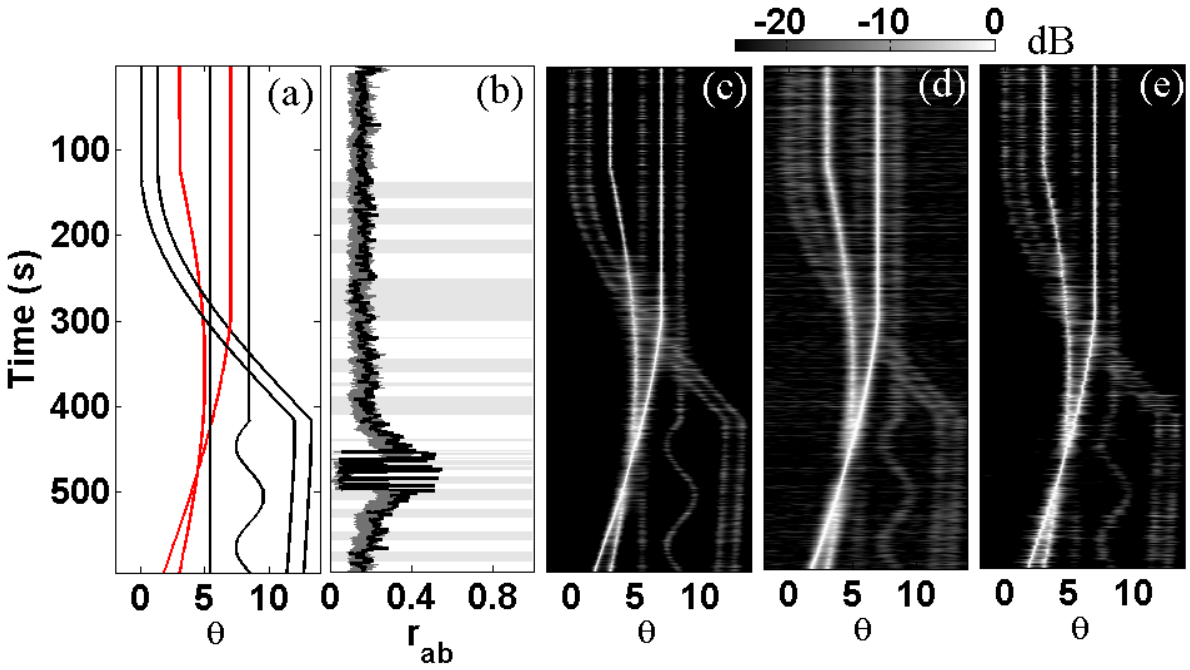

Figure 3 Example of eigenspace stationarity in simulated data:[10] (a) Time-dependent azimuth of six maneuvering targets (red=loud sources); (b) Stationarity metric r_{ab} (solid black line) compared to theoretical bounds (dark grey box). Horizontal boxes indicates segments of data deemed as stationary according to the criterion in eq.(6); (c) $BF_{Ma}^{(true)}$ (d) $BF_{Ma}^{(M_o=M)}$ with $M_o = 10$ snapshots; (e) $BF_{Ma}^{(M_o \geq M)}$, with $M_o \geq 10$ snapshots according to the stationarity segments in (b).

The stationarity-aided beamforming approach was also applied to experimental data from the CalOps portion of the Shallow Water Array Performance (SWAP) experiment.[14] Although a towed active source was utilized during CalOps experiment,[14] analysis of the full data set is still ongoing and in this report we only consider data segments with sources of opportunity (shipping traffic). Beamforming results for data collected on September 7th, 2007 are shown in Fig. 4. The data was collected on a 100-sensor horizontal line sub-array, for a total 175 m aperture. Figure 4(a) shows the application of the stationarity metric to the dominant time-varying eigenspace. Similar to the previous simulated example, r_{ab} exhibits variability due to the lack of snapshots used to compute the eigenspaces at each time, as well as due to true variations in the underlying data statistics from surface ship movement. Figure 4 (b) shows $BF_{Ma}^{(M_o=M)}$ for $M_o = 5$ snapshots, allowing the detection of multiple targets in the watercolumn. Improved results $BF_{Ma}^{(M_o \geq M)}$ are shown Fig.4(c), which exhibit reduced background noise levels and better detection capabilities of quiet targets than panel (b).

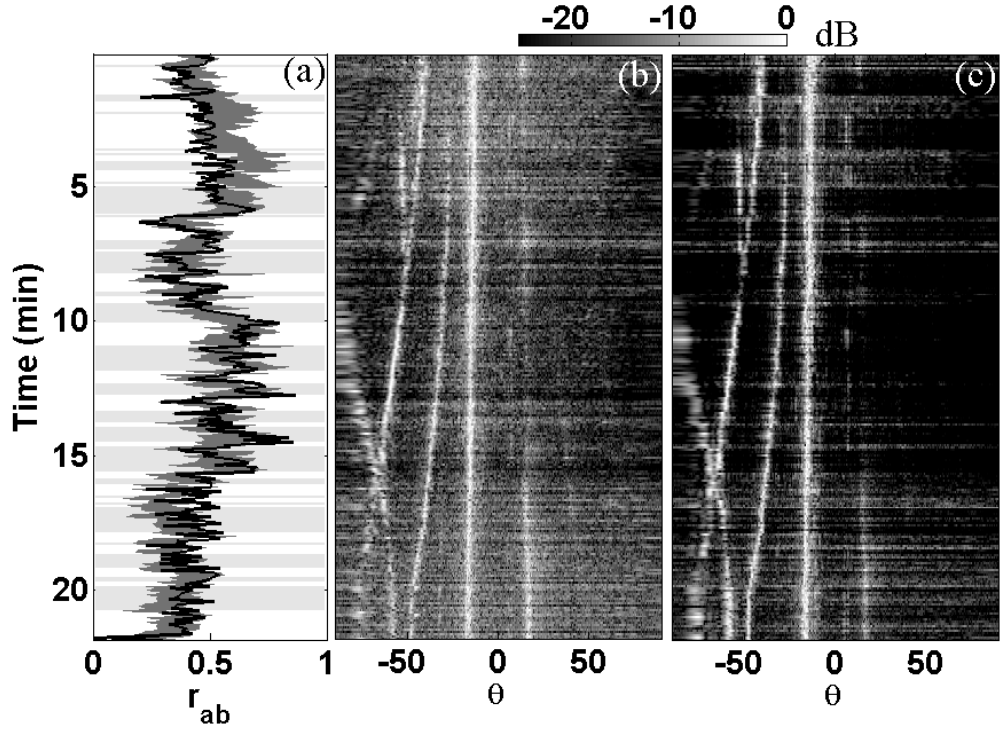

Figure 4 Eigenspace stationarity[10] applied to experimental data from the SWAP experiment.[14] The data was collected at a 100-sensor horizontal line sub-array, at 415 Hz. (a) Stationarity metric r_{ab} (solid black line) compared to theoretical bounds (dark grey box). Horizontal boxes indicates segments of data deemed as stationary; (b) $BF_{Ma}^{(M_o=M)}$ with $M_o = 5$ snapshots; (c) $BF_{Ma}^{(M_o \geq M)}$, with $M_o \geq 5$ snapshots according to the stationarity segments in (a).

2) Eigenvector-based beamforming (EVB):[10] as illustrated in Fig.3, eigenvectors with information content related to targets in the watercolumn exhibit different statistical properties to those related to background noise. In this research we propose an eight-step algorithm that exploits this information content to estimate the signal subspace for data projection prior to beamforming:

Estimating the eigenbasis $\overline{\mathbf{u}}_k$ required for the proposed EVB beamformer:

Step 1: Given *M* data snapshots, compute the sample eigenvectors $\hat{\mathbf{u}}_1,...,\hat{\mathbf{u}}_M$.

Step 2: Compute the steering vectors $\mathbf{v}(\theta_f)$ for a fine grid of steering angles $-90^o \leq \theta_f \leq 90^o$.

Step 3: Define T_F as the solution of $F = \int_{\alpha_{\min}=0}^{T_F} f_{\alpha_{\min}}(\alpha_{\min}) d\alpha_{\min}$, where *F* is a user-defined constant $0 \leq F \leq 1$. Notice that F is ultimately related to the percentage of false detections at the output of the proposed beamformer. For example, *F=0* results in 0 informative eigenvectors (i.e., no false alarms, but also misses all true detections), while *F=1* indicates that all eigenvectors are informative, leading to large number of false alarms.

Step 4: Initialize $\mathbf{s}_k = \hat{\mathbf{u}}_k$ for $k = 1..M$.

Step 5: Find θ_f for which $\text{acos}\left(|\mathbf{s}_k^H \mathbf{v}(\theta_f)|\right) < T_F$.

Step 6: Remove $\mathbf{v}(\theta_f)$ from $\mathbf{s}_k$ as: $\mathbf{s}_k = \mathbf{s}_k - |\mathbf{s}_k^H \mathbf{v}(\theta_f)|\,\mathbf{v}(\theta_f)$ for $k = 1..M$.

Step 7: Repeat from step 5 until $\text{acos}\left(|\mathbf{s}_k^H \mathbf{v}(\theta_f)|\right) \geq T_F$ for all θ_f.

Step 8: The resulting non-orthogonal vectors $\mathbf{g}_k = \hat{\mathbf{u}}_k - \mathbf{s}_k$ (where $k = 1..M$), span the signal eigenspace. Applying singular value decomposition to $\mathbf{g}_k$ gives the orthonormal basis $\overline{\mathbf{u}}_k$, where $k = 1...\overline{Q}$ and $\overline{Q}$ is automatically determined by the column rank of $\mathbf{g}_k$.

Notice that the main idea behind this algorithm is the removal of plane-wave wavefronts from the sample eigenvectors (step 6). Selecting which wavefronts are to be removed is done based on the criterion in step 5. By step 8, $\mathbf{s}_k$ spans the noise subspace while $\mathbf{g}_k$ spans the signal subspace.
The eigenvector-based beamformer described in Table 1 was applied to simulated data by projecting the data into the $\overline{\mathbf{u}}_k$ basis estimated by the previous algorithm. An example of this result is shown in Fig.5, in which 120 Monte Carlo beamforming realizations were obtained for an experimental scenario consisting of a 100-sensor horizontal line array in the presence of 6 sources with azimuth $0^o, 1.3^o, 3^o, 5.5^o, 7^o, 3^o$, and 8^o. Each Monte Carlo realization consists of generating *M=10* data snapshots and applying adaptive beamforming. Figure 5 (a) shows $BF_{Ma}^{(M_o=M)}$ (i.e., the traditional MVDR result). Figure 5 (b) shows the proposed $BF_{Ma}^{(EVB)}$ obtained by using a threshold $F = 0.05$ (see step 3 in previous algorithm). A detailed view of the beamforming results is shown in Fig.5(c) for a single Monte Carlo realization. In this case, $BF_{Ma}^{(EVB)}$ (red line) accurately detects five out of six targets, missing the one at 1.3^o. In addition, an evident false detection can be seen at -43^o. However, $BF_{Ma}^{(EVB)}$ yields sharper detections that allow clear view of the number of sources used in the simulation. Ongoing research on the proposed eigenvector-based beamformer is on relating the user-selected value of F to the percentage of false detections at the beamformer output, in such a way to provide a guaranteed false alarm rate.

Figure 6 shows[10] a comparison between MVDR(Fig.6 (a)) and EVB (Fig.6 (b) and (c)) beamformers applied to experimental data from the SWAP experiment.[14] The results for EVB were computed using two false detection levels: with $F = 0.05$ in (b) only the most prominent targets are visualized, yielding fewer false detections compared to $BF_{Ma}^{(M_o=M)}$ in (a). As in the simulated case, target detections are sharp, suggesting an improved azimuth resolution. By increasing the false detection level to $F = 0.1$, the number of target-related detections increases at the expense of a higher number of false peaks. However, even in this case EVB significantly reduces the number of false detections when compared to MVDR in Fig.6 (a). Details of the improvement in azimuth resolution of the EVB beamforming are shown Fig.7, which corresponds to a zoom-in view of the results in Fig.6.

IMPACT/APPLICATIONS

This work will benefit adaptive beamforming techniques, in particular algorithms that rely on accurate estimation of covariance matrices, matrix rank, and subspaces. This research aims to enhancing the sensitivity to detect genuine variations (trends) in signal statistics, by applying results from a growing body of research on the asymptotic behavior of eigenvectors of sample covariance matrices.[3-8] This research provides: data-driven bounds for data segmentation based on data stationarity and improved estimators of signal vs noise subspaces of a sample covariance matrix computed from few snapshots.

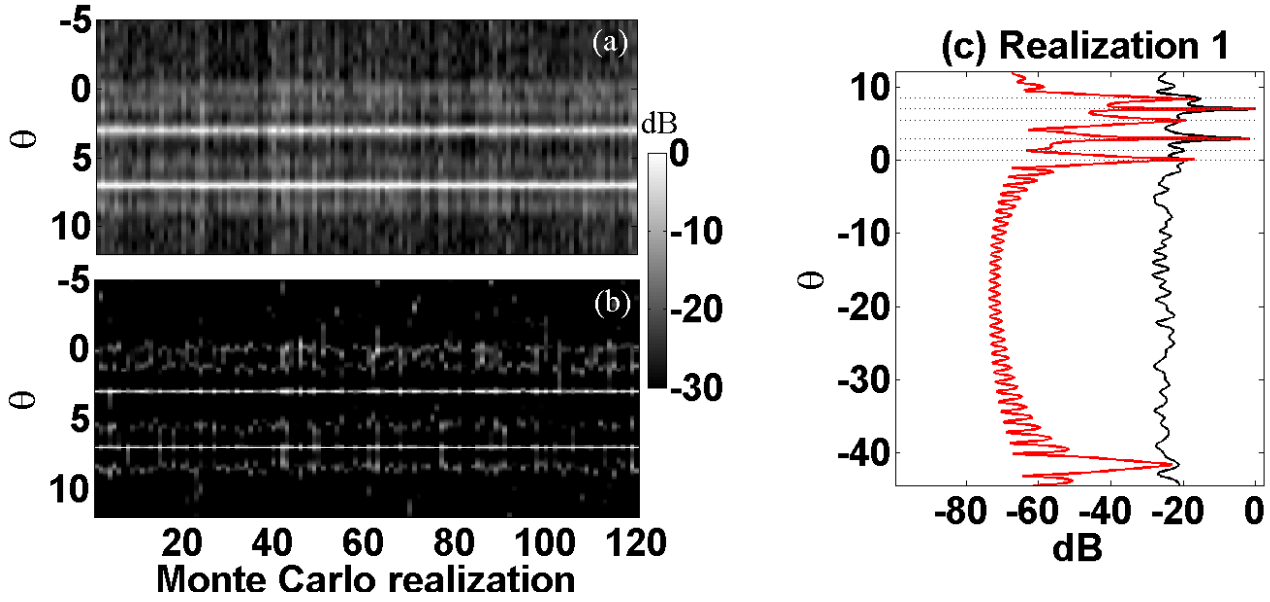

Figure 5 Improved beamforming by exploiting sample eigenvector signal content:[10] (a) MVDR beamformer $BF_{Ma}^{(M_o=M)}$ ***using*** $M=10$ ***snapshots/Monte Carlo realization; (b) Proposed eigenvector-based beamformer*** $BF_{Ma}^{(EVB)}$ ***; (c)*** $BF_{Ma}^{(M_o=M)}$ ***(black line) versus*** $BF_{Ma}^{(EVB)}$ ***(red line) for the first Monte Carlo realization in (a) and (b). Horizontal dashed lines indicate the azimuth of the six sources used in this simulation.***

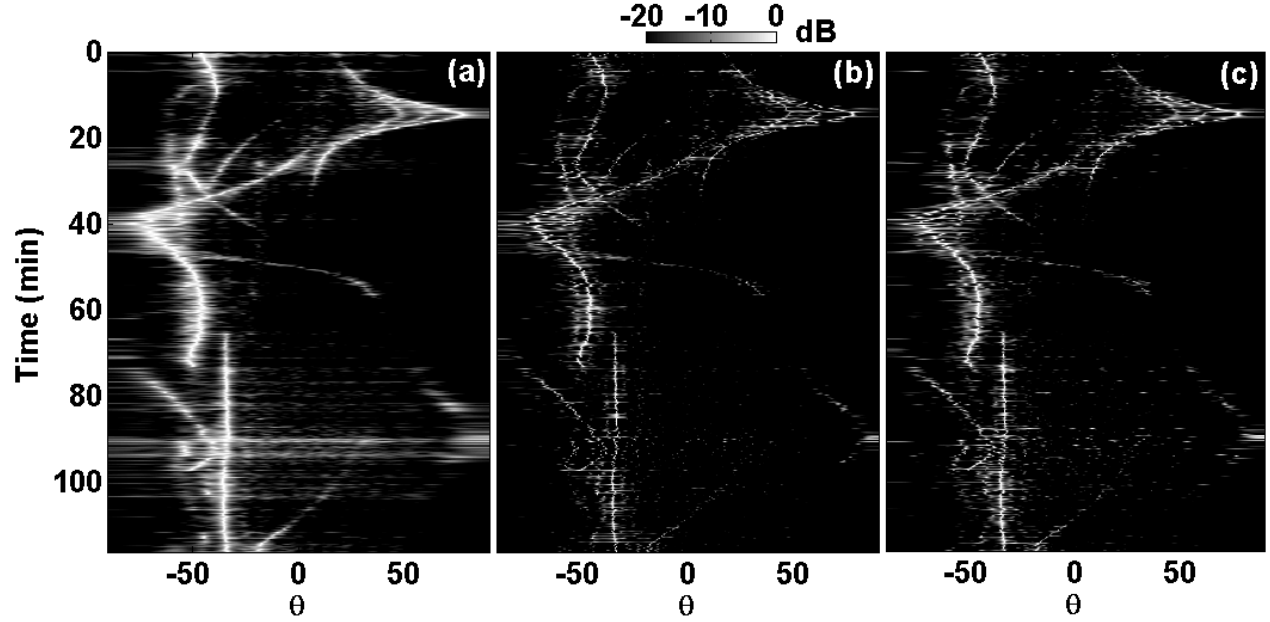

Figure 6 Eigenvector-based (EVB) beamforming applied to experimental data (f=205 Hz) from the SWAP experiment collected at a sub-array with N=60 hydrophones:[14] (a) MVDR beamformer $BF_{Ma}^{(M_o=M)}$ ***using*** $M=10$ ***snapshots; (b)*** $BF_{Ma}^{(EVB)}$ ***with false detection level*** $F=0.05$ ***; (c)*** $BF_{Ma}^{(EVB)}$ ***with*** $F=0.1$***. For comparison between beamformers, results are normalized with maximum corresponding to 0 dB.***

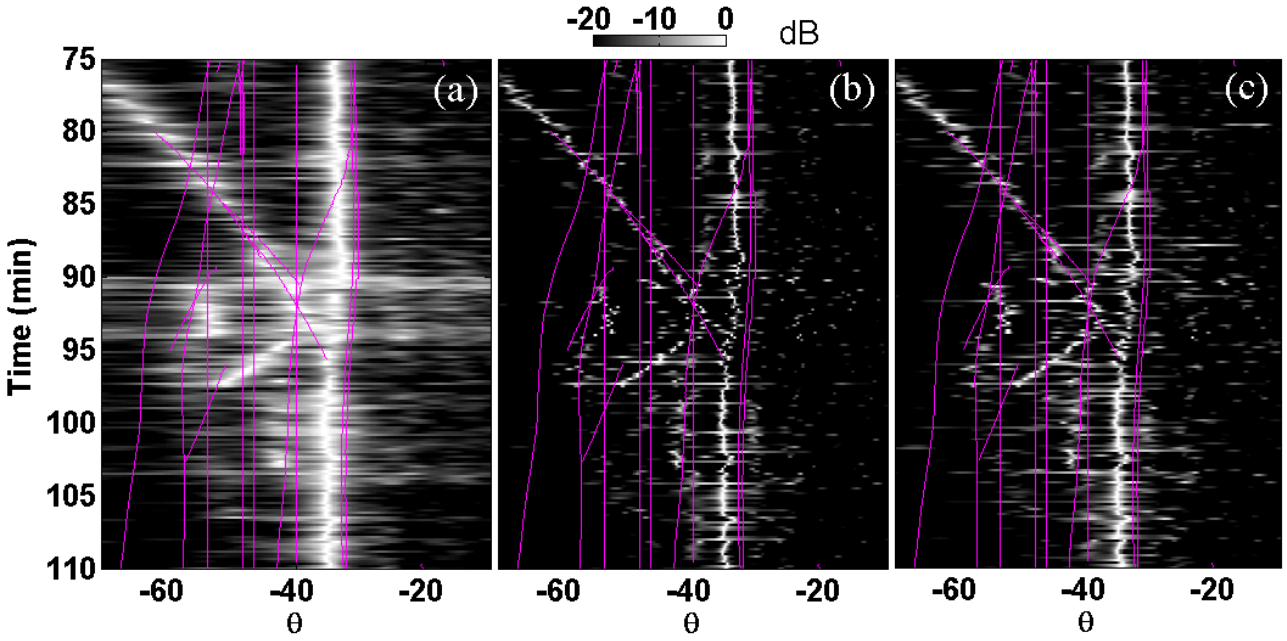

Figure 7 Zoom-in view of Fig.6, showing the improved azimuth resolution obtained by the EVB beamformer in (b) and (c) compared to the MVDR beamformer in (a). Over plotted lines indicate actual ship lanes obtained from AIS data collected during the SWAP experiment. [14]

RELATED PROJECTS

None.

REFERENCES

[1] Song, H., Kuperman, W.A., Hodgkiss, W.S., Gerstoft, P. and Kim, J.S., "Null broadening with snapshot-deficient covariance matrices in passive sonar", IEEE J. of Oceanic Eng. 28, pp.250-261 (2003).

[2] Baggeroer, A.B. and Cox, H., "Passive sonar limits upon nulling multiple moving ships with large aperture arrays", Proc. 33rd Asilomar Conference in Signals, Systems and Computers, IEEE Computer Society, pp.103-108 (1999).

[3] Paul, D., "Asymptotics of sample eigenstructure fo a large dimensional spiked covariance model", Statistica Sinica 17, pp. 1617-1642 (2007).

[4] Mestre, X., "On the asymptotic behavior of the sample estimates of eigenvalues and eigenvectors of covariance matrices", IEEE Trans. On Signal Processing 56, pp. 5353-5368 (2008).

[5] Nadakuditi, R., and Edelman, A., "Sample eigenvalue based detection of high-dimensional signals in white noise using relatively few samples", IEEE Trans. on signal processing 56, pp.2526-2638 (2008).

[6] Benaych-Georges, F., and Nadakuditi, R., "The singular values and vectors of low rank perturbations or large rectangular random matrices", Journal of Multivariate Analysis 111, pp. 120-135 (2012).

[7] Lee, S., Zou, F., and Wright, F. A., "Convergence and prediction of principal component scores in high-dimensional settings", Ann. Statist. 38, pp. 3605-3629 (2010).

[8] Jung, S., Sen, A., and Marron**,** J. S. "Boundary behavior in high dimension, low sample size asymptotics of PCA", Journal of Multivariate Analysis", vol. 109, pp. 190-203 (2012).

[9] Quijano, J. E., and Zurk, L. M., "An eigenvector-based test for local stationarity applied to array processing", JASA 135, 2014.

[10] Quijano, J. E., and Zurk, L. M., "Analysis of Eigenspace Dynamics for Adaptive Nulling with Moving Interference", ONR SP program review, August 2014.

[11] Allez, R., and Bouchaud, J., "Eigenvector dynamics: General theory and some applications", American Physical Society Physical Review 86, pp. 1-23 (2012).

[12] Cai, T., Liu, W., and Xia, Y., "Two-sample covariance matrix testing and support recovery in high-dimensional and sparse setting", Journal of the American Statistical Association 108, pp. 265-277 (2013).

[13] Berger, T., "On the correlation coefficient of bivariate, equal variance, complex Gaussian sample", Annals of Math. Stat. **43**, 1972.

[14] Heaney, K.D., and Murray, J. J., "Measurements of three-dimensional propagation in a continental shelf environment", J. Acoust. Soc. Am. **125**, pp. 1394-1402, 2009.

PUBLICATIONS

Quijano, J. E., and Zurk, L. M., "An eigenvector-based test for local stationarity applied to array processing", JASA 135, 2014.